

Thermal Ductility and Hot Cracking for 70 mm Thick Forge Plate and Rolling Plates of Nickel Alloy 690

Jiang Yunlu¹, Chen Huaining¹, Wu Changzhong¹, Chi Yunfei²

¹ CAS Key Laboratory of Nuclear Materials and Safety Assessment, Institute of Metal Research, Chinese Academy of Sciences, Shenyang 110016, China; ² Harbin Electric Corporation (Qinhuangdao) Heavy Equipment Co. Ltd, Qinghuangdao 066206, China

Abstract: The thermal ductility and hot cracking sensibility of the forge and the rolling plates with 70 mm in thickness were studied by optical microscope (OM), scanning electron microscope (SEM), and Gleeble 1500 thermal simulation equipment. The results show that the forge and the rolling plates both have excellent thermal ductility; the samples taken from surface position present higher thermal ductility than those taken from middle position of the same plate. During the heating process, the rolling plate has higher thermal ductility than the forge plate at the lower temperature. With the increase of the temperature, the forge plate is characterized by higher thermal ductility compared with the rolling plate. However, during the cooling process, the forge plate indicates higher thermal ductility than the rolling plate. The fracture position features more smoother morphology, even the melt phenomenon exists at some positions. Besides, high hot cracking sensitivity appears in both the forge and rolling nickel alloy 690. And the crack number and length increase with the applied strain increasing.

Key words: nickel alloy 690; thermal ductility; hot cracking

Nuclear facilities serve perennially service in the high temperature, high pressure and radial environment of nuclear station. The fabrication materials for nuclear station shall have the characteristic of high temperature ductility and hot cracking resistance in order to ensure safety and reliable operation^[1-3]. As one of the most promising candidate materials for super-critical water reactor (SCWR), nickel alloy 690 has superior resistance to intergranular stress corrosion cracking (IGSCC) and intergranular corrosion (IGC) in various environments^[4-6]. Alloy 690 is applied to manufacture the key components in nuclear plants, such as nuclear pressurized water nuclear reactors and steam generator^[7]. However, it has been pointed out that alloy 690 is susceptible to hot cracking under heavy restraint conditions such as welding thick components. As for its nature, hot cracks mainly include the solidification crack and the ductility-dip crack (DDC).

The brittle temperature range (BTR) or the formation

temperature range of solidification crack depends upon the range of a solid-liquid state of metal in the solidification of the weld. The lower limit of this range is determined by the value of solidus temperature at the end of solidification^[8].

DDC is a solid-state hot crack, caused by grain boundary embrittlement at the homologous temperature that ranges from about 0.5 to 0.8 of the alloy melting points, which is observed at grain boundaries^[3,9-11]. This ductility drop may result in intergranular elevated temperature cracking, often referred to as (DDC)^[12]. DDC may occur during the high temperature processing of these alloys or during welding if the imposed strain exhausts the available ductility within this temperature range^[3,13].

There are many important indexes conducted in nuclear materials, such as the irradiation embrittlement for metal components in primary circuit. The aim of the paper is to study the thermal ductility and hot cracking features of 70 mm thick forge and rolling plates of nickel alloy 690 by

Received date: March 10, 2018

Corresponding author: Chen Huaining, Ph. D., Researcher, Institute of Metal Research, Chinese Academy of Sciences, Shenyang 110016, P. R. China, E-mail: hnchen@imr.ac.cn

Copyright © 2019, Northwest Institute for Nonferrous Metal Research. Published by Science Press. All rights reserved.

thermal simulation and experiments. Further, the results in the study may contribute to the database of nuclear industry.

1 Experiment

The 70 mm thick experimental alloy 690 plates used in this paper were forged and rolled in the thickness direction. Its chemical composition is shown in Table 1 and mechanical properties is shown in Table 2. The final heat treatment was solution and age heat treatment. The samples taken from the surface and the middle of the forge plate and the rolling plate were abbreviated to FS, PS, FM and PM, respectively. Fig.1 shows the OM images of the samples FM and PM.

The thermal ductility was analyzed by the thermal simulation equipment Gleeble 1500. The samples with a size of $\phi 6 \text{ mm} \times 115 \text{ mm}$ were taken from the surface and middle of the both plates of nickel alloy 690. The differential thermal analysis (DTA) tests were carried out on an SETSYS Evolution18 integrated thermal analyzer developed by SETARAM Corporation. During the test the samples were first heated to 1100 °C at a rate of 80 °C/min, and then heated continuously to 1450 °C at a rate of 10 °C /min. The initial melting point was measured through the first peak on the melting curve. Fig.2 shows the DTA test results for the rolling plate. The simulated thermal ductility process includes the heating and cooling processes. During the heating process the samples were heated to specified peak temperature and held for 0.5 s, and then quickly stretched at a speed of 20 mm/s. During the cooling process the samples were heated to 1350 °C peak temperature, held for 0.5 s, then cooled to the specified temperature at cooling rate of

50 °C/s and subsequently held for 0.5 s, and finally quickly stretched at a speed of 20 mm/s.

The Varestain test was used to evaluate transverse hot cracking sensitivity of nickel alloy. The samples were taken from the surface and middle of the 70 mm thick forge and rolling plates of nickel alloy 690 with a size of 320 mm \times 80 mm \times 8 mm. During the test, the samples were forced to different external strains, while welding to the center position of the samples. Mechanical grinding and polishing were applied to prepare the samples for microstructure observation, followed by etching using a 5 g CuSO₄+20 mL HCl +20 mL H₂O reagent for 20~30 s. The microstructures were observed by optical microscope (OM), and scanning electron microscope (SEM).

2 Results and Discussion

2.1 Thermal ductility

Fig.3 shows the thermal ductility of the forge and the rolling plates of nickel alloy 690. As shown in Fig.3, the rolling plate has higher thermal ductility than the forge plate at lower temperature (lower than 1200 °C) during the heating process. With the increase of the temperature (higher than 1300 °C), the forge plate has higher thermal ductility than the rolling plate. The samples taken from surface plate have higher thermal ductility than those from middle position in the same plate. During the cooling process, the forge plate shows higher thermal ductility than the rolling plate, especially the samples taken from the surface of the forge plate which show existing an excellent thermal ductility than others.

Table 1 Chemical composition of alloy 690 (wt%)

Element	C	Si	Mn	S	P	Mg	Cr	Al	Ti	Fe	Ni
Forge plate	0.027	0.15	0.38	0.002	0.003	0.001	29.22	0.1	0.23	8.9	Bal.
Rolling plate	0.02	0.29	0.3	<0.001	<0.005	0.0019	29.04	0.18	0.21	10.2	Bal.

Table 2 Mechanical properties of alloy 690

Mechanical properties	$R_{p0.2}$ /MPa	R_m /MPa	δ /%	ψ /%
Forge plate	250	599	60	58
Rolling plate	245	625	55	63

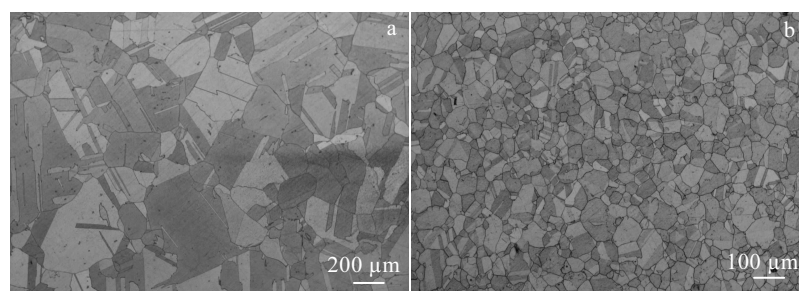


Fig.1 Optical micrographs of middle position of plates: (a) the forge plate and (b) the rolling plate

The tendency of hot cracking is always related to the thermal properties, such as Nil-strength temperature (NST), Nil-ductility temperature (NDT), Nil-ductility range (NDR) and brittleness temperature range (BTR). Those parameters play crucial roles in the hot cracking, and can be summarized from Fig.3 and shown in Table 3. The rolling plate shows higher Nil-strength temperature and Nil-ductility temperature than the forge plate in heating process. However, Nil-ductility temperature is the same for both plates in cooling process. Therefore, the rolling plate has wider Nil-ductility range and Brittleness temperature range than the forge plate.

2.2 Fracture morphology of thermal ductility

Fig.4 and Fig.5 show the fracture morphologies of the samples during the heating process at 1300 °C. A high thermal ductility exists in the heating process, as shown in Fig.4. The reduction in the area can reach 72% for the sam-

ple from the surface position of rolling plate. Fig.5 shows the SEM morphology of the fracture positions. The fracture positions were characterized by smooth morphology, even the melt phenomenon was observed in some positions.

Fig.6 and Fig.7 show the fracture morphologies of the cooling process at 1300 °C. High thermal ductility is also found in the cooling process, as shown in Fig.6. In particular, the sample reduction of the area can reach 62% at the middle position of the forge plate; however the thermal ductility sharply decreases after the thermal circle of the sample PS. Fig.7 shows SEM morphologies of the fracture positions. The fracture positions present smooth morphology, and some positions exhibit the melt phenomenon. The melt phenomenon may arise from the high peak temperature. Some dimples are distributed in the fracture position of the sample FM.

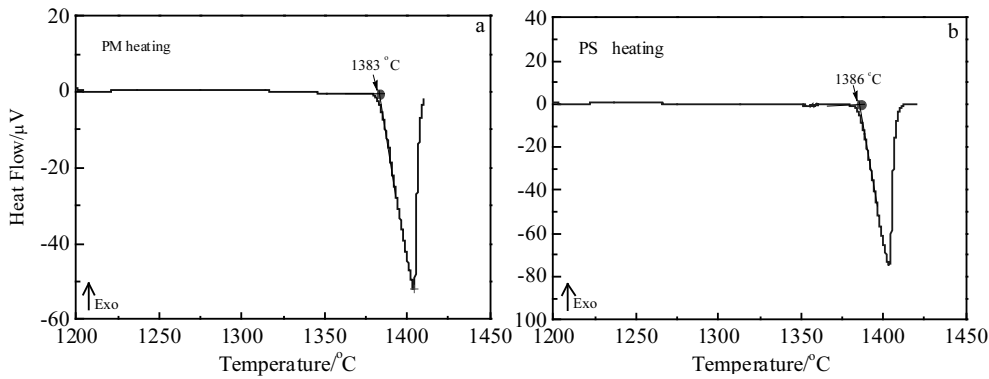


Fig.2 DTA test results of PM (a) and PS (b)

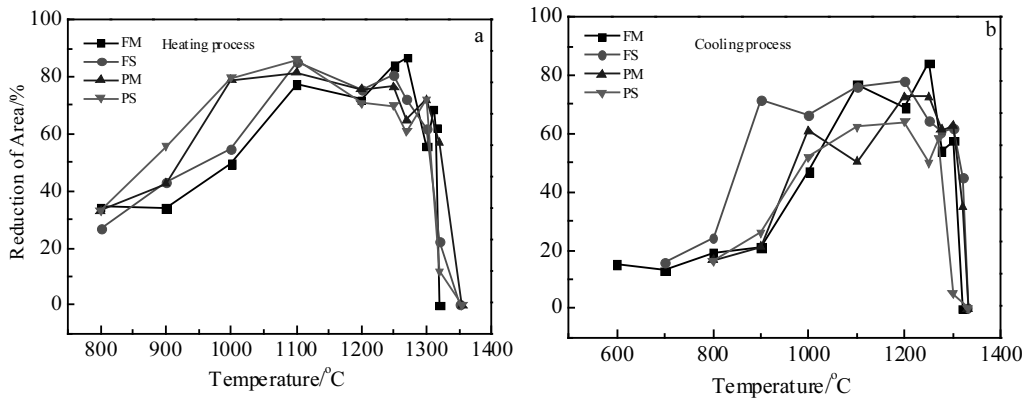


Fig.3 Thermal ductility during the heating (a) and cooling (b) processes

Table 3 Thermal properties of alloy 690

Sample number	Nil-strength temperature (NST)/°C	Nil-ductility temperature (NDT)-heating/cooling process/°C	Nil-ductility temperature range (NDR)/°C	Brittleness temperature range (BTR)/°C
FM	1356	1350/1330	20	26
FS	1352	1345/1330	15	22
PM	1363	1355/1330	25	33
PS	1360	1355/1330	25	30

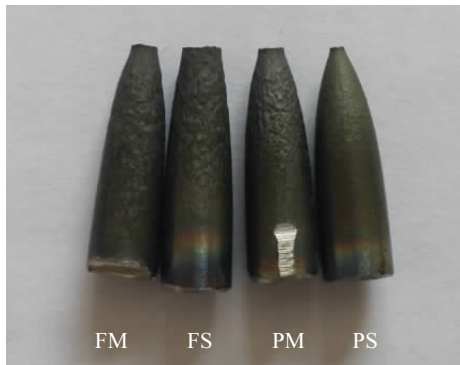


Fig.4 Macroscopical fractures during the heating process

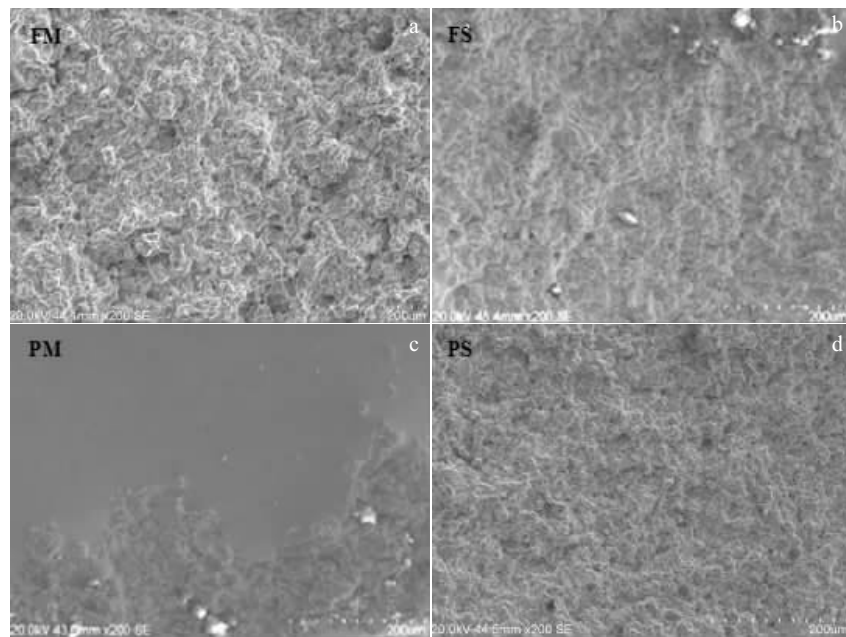


Fig.5 Fractures morphologies during the heating process: (a) FM, (b) FS, (c) PM, and (d) PS



Fig.6 Macroscopical fractures during the cooling process

Similar cavity-like feature was identified on the fracture surfaces in the heating process, as shown in Fig.8. The fracture surfaces and cavities are clearly intergranular even though some oxides are covered. Moreover, discontinuous cavities along the secondary crack of the fracture surface are observed as shown in Fig.8. There is no doubt that all these cavities are evidence of weakness zone during the crack growth, indicating that cavities play an important role in the crack propagation in thermal ductility during the heating process.

2.3 Varestain test

The Varestain test was used to evaluate the transverse hot cracking sensitivity of nickel alloy 690 which is shown in Fig.9. The variably strain was obtained by the different

radius curvature modules of the welded samples. The tensile strain may be varied by:

$$\varepsilon = \frac{\delta}{2R} \times 100\% \quad (1)$$

Where ε is the strain of the sample, δ is the thickness of the sample, and R is the radius curvature of the module. Tungsten inert gas welding was used to weld on the surface of samples. The welding direction is from the position A to the position C. The given tensile strain was forced on the samples while the welding went to the central position B. The welding parameters are as follows: welding current 200 A, welding voltage 14~16 V, welding speed 2~3 mm/s. Fig.9 shows the schematic diagram of Varestain test.

The surface cracks were inspected by a liquid penetrating test. The maximum length and total length of cracks are shown in Fig.10. From the results, it can be summarized that the forge or rolling nickel alloy 690 plate has high hot

cracking sensitivity, and critical cracking strain is only 0.8% to 1%. The crack number and length both increase with the strain level.

The four cracking positions are shown in Fig.11 from the sample with the strain of 1%. The depth of the crack is often over 1 mm. The cracks are not only generate on the surface of samples, but also appear inside the samples. The cracking direction is vertical to the loading strain.

3 Discussion

Generally, because of the differences between deformation and microscopic structure for the thermal ductility and weldability, some differences between the nickel alloy 690 with a thickness of 70mm are possibly found, which are caused by forging and rolling. Otherwise, with a thickness of 70mm, following the traditional process conditions, some differences in surface and middle position still exist.

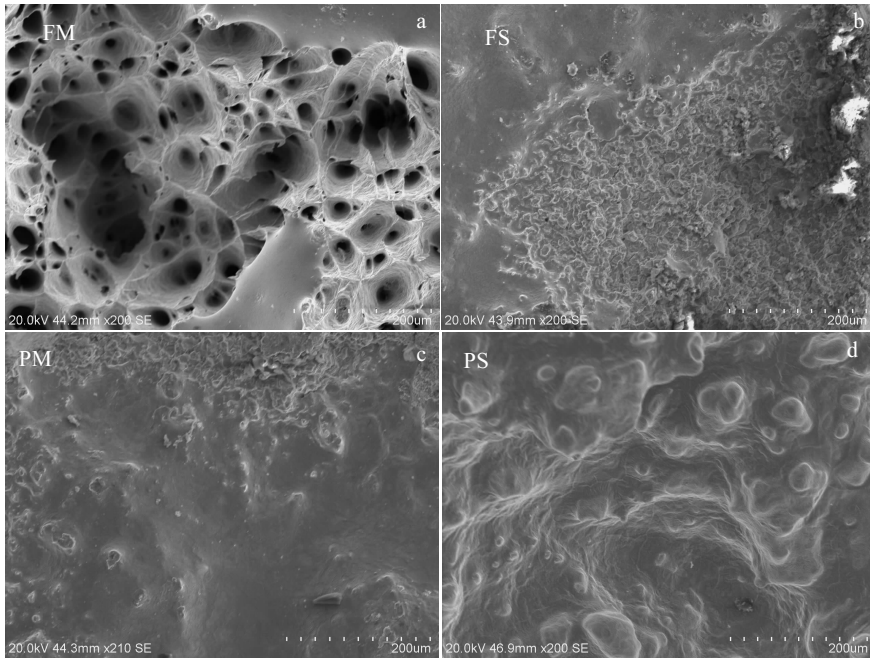


Fig.7 Fracture morphologies during the cooling process: (a) FM, (b) FS, (c) PM, and (d) PS

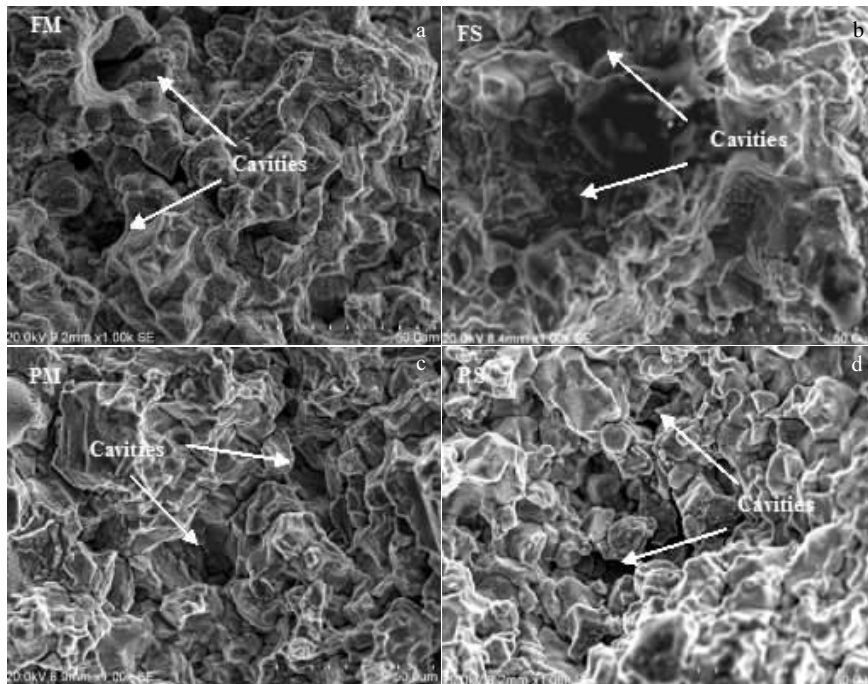


Fig.8 Magnified fracture morphologies during the heating process: (a) FM, (b) FS, (c) PM, and (d) PS

The result shows clearly that the grain size of the forge plate is one magnitude larger than that of rolling plate (as shown in Fig.1), but whether forge or rolling plate is used, there is no significant difference between the grain size and microscopic structure in surface and middle positions. This helps us get a conclusion that the material properties of the surface and the middle positions are nearly the same. This

is possibly due to the strengthening elements of the forge plate and the forging process, which can lead to the fact that the grain size of the forge plate is one magnitude larger than that of the rolling plate, but the similar mechanical property is observed.

Few differences in the thermal ductility are observed for both the forge and rolling plates, including NST, NDT,

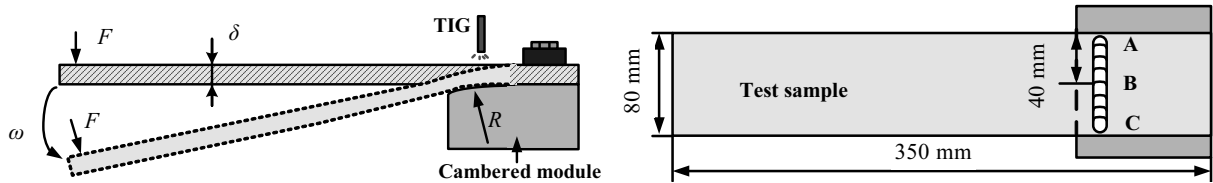


Fig.9 Schematic diagram of Varestain test

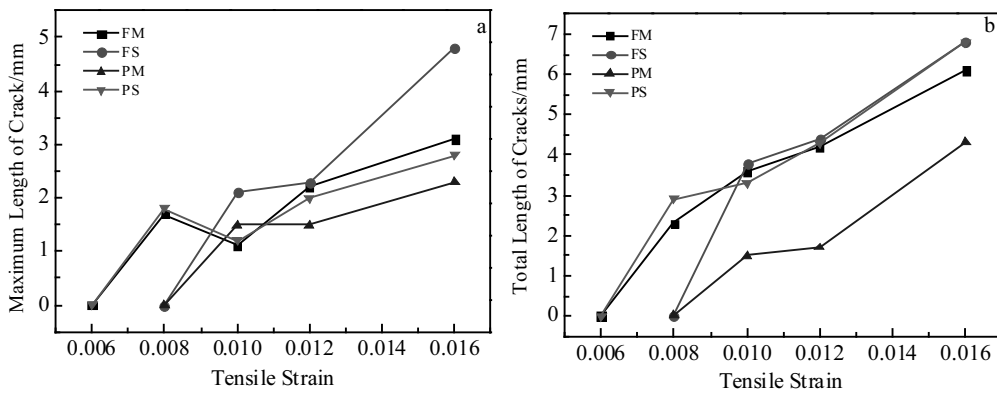


Fig.10 Crack counts on the sample surface: (a) maximum crack length vs tensile strain and (b) total crack length vs tensile strain

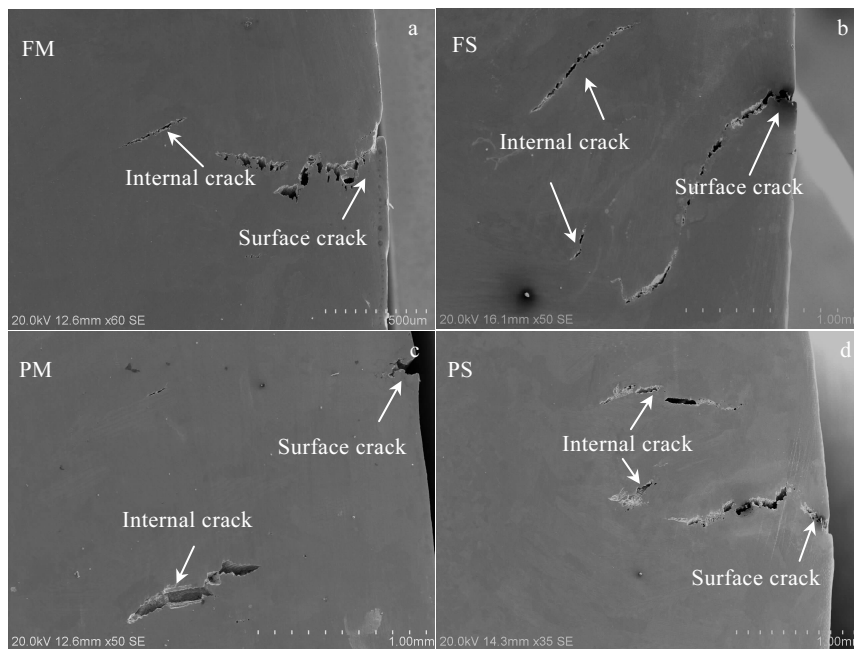


Fig.11 Cracking section of the samples FM (a), FS (b), PM (c) and PS (d)

NDR and BTR. Also, similar results appear for the hot cracks sensitivity, which is one of the most important indicators of the weldability. Those indicate that the grain size that affects the conventional mechanical property has little effect on the thermal ductility and hot cracking sensitivity.

The morphology show that cavity features on the fracture surface as clear evidence of hot cracking. The hot cracking is influenced by the liquid phase of nickel alloy in high temperature process. These cavities which nucleate around grain boundary, probably result from the condensation of liquid phase. At the same time, the low melt point impurity is easy to gather in grain boundary, such as phosphorus and sulphur. Those cavities and liquid phase are sensitivity position when suffering from loading. Therefore, the grain boundary exists as the source of initiation crack in high temperature tension.

4 Conclusions

1) The forge and rolling plates of the nickel alloy 690 have high thermal ductility at high temperature. The fracture positions present smooth morphology, even some positions featuring the melt phenomenon.

2) The forge and rolling plates of the nickel alloy 690 both have high cracking sensitivity. The number and length of crack increase with the tensile strain level. The depth of crack is over 1 mm. The cracks are always generated on the surface and interior of the samples. The cracking direction is almost vertical to that of loading strain.

3) Few differences are presented for the thermal ductility

and hot cracking sensitivity of the forge and the rolling plates.

References

- 1 Li Y H, Wang J Q, Han E H et al. *Acta Metallurgica Sinica*[J], 2012, 48(8): 941
- 2 Ramirez A J, Lippold J C. *Materials Science and Engineering A*[J], 2004, 380: 259
- 3 Ramirez A J, Lippold J C. *Materials Science and Engineering A*[J], 2004, 380: 245
- 4 Cheung C, Erb U, Palumbo G. *Materials Science and Engineering A*[J], 1994, 185(1-2): 39
- 5 Hou J, Shoji T, Lu Z P et al. *Journal of Nuclear Materials*[J], 2010, 397(1-3): 109
- 6 Lee H T, Wu J L. *Corrosion Science*[J], 2009, 51(4): 733
- 7 Kuang W J, Gary S. Was, Cody Miller et al. *Corrosion Science*[J] 2018, 130: 126
- 8 Yushchenko, V. Savchenko, N. Chervyakov et al. *Welding in the World*[J], 2011, 55(9-10): 28
- 9 Nishimoto K, Saida K, Okauchi H. *Science and Technology of Welding and Joining*[J], 2006, 11(4): 455
- 10 Qin R Y, Duan Z L, He G. *Metallurgical and Materials Transactions A*[J], 2013, 44(10): 4661
- 11 Mo W L, Lu S P, Li D Z et al. *Materials Science and Engineering A*[J], 2013, 582: 326
- 12 Saida K, Ohta K, Nishimoto K. *Science and Technology of Welding and Joining*[J], 2007, 12(7): 593
- 13 Mo W L, Hu X B, Lu S P et al. *Journal of Materials Science & Technology*[J], 2015, 31: 1258

70 mm 厚锻造及轧制镍基合金 690 板材热塑性和热裂纹敏感性

姜云禄¹, 陈怀宁¹, 吴昌忠¹, 池云飞²

(1. 中国科学院 核用材料与安全评价重点实验室 (中国科学院金属研究所), 辽宁 沈阳 110016)

(2. 哈电集团 (秦皇岛) 重型装备有限公司, 河北 秦皇岛 066206)

摘要: 利用光学显微镜、扫描电镜及 Gleeble 1500 热模拟机, 分析 70 mm 厚锻造及轧制镍基合金 690 板材的热塑性及热裂纹敏感性。结果表明: 锻造和轧制板材均有优异的热塑性, 同种材料试样表层的热塑性高于试样中心位置的热塑性。模拟加热过程发现, 较低温度条件下轧制板材的热塑性高于锻造板材的热塑性, 随着温度的升高锻造板材的热塑性高于轧制板材的热塑性。模拟冷却过程发现, 锻造板材比轧制板材具有更好的热塑性。热模拟试样的断面较为光滑, 部分位置出现熔融现象。横向可调拘束裂纹敏感性试验结果显示, 锻造及轧制镍基合金 690 板材具有较高的热裂纹敏感性。随着施加应变的增大, 热裂纹的数量增多且长度增加。

关键词: 镍基合金690; 热塑性; 热裂纹

作者简介: 姜云禄, 男, 1986 年生, 硕士, 助理研究员, 中国科学院金属研究所, 辽宁 沈阳 110016, 电话: 024-23971932, E-mail: yljjiang@imr.ac.cn